Scientia Iranica C (2022) 29(3), 1338–1350

Sharif University of Technology
Scientia Iranica
Transactions C: Chemistry and Chemical Engineering
http://scientiairanica.sharif.edu

Copper (II) supported on a post-modified magnetic pectin Fe_3O_4@Pectin∼Imidazole∼SO_3H-Cu(II): An efficient biopolymer-based catalyst for selective oxidation of alcohols with aqueous TBHP

P. Ghamari Kargar, M. Ghasemi, and Gh. Bagherzade*

Department of Chemistry, Faculty of Sciences, University of Birjand, Birjand, P.O. Box 97175-615, Iran.

Received 17 May 2021; received in revised form 14 July 2021; accepted 23 August 2021

KEYWORDS
Magnetic nanoparticle;
Pectin;
Biopolymer;
Copper complex;
Oxidation;
Benzyl alcohol.

Abstract. Designing a catalyst that combines activity, selectivity, and simple recovery as well as follows green chemistry instructions is of great importance. In the present study, Fe_3O_4@Pectin∼Imidazole∼SO_3H-Cu(II) was synthesized as an efficient and biopolymer-based magnetic catalyst for the oxidation of benzyl alcohols to aldehydes using tert-butyl hydroperoxide as an oxidant under solvent-free conditions. The catalyst was characterized using Fourier transform infrared spectroscopy, powder X-ray diffraction, vibrating sample magnetometer, field emission scanning electron microscopy, energy dispersive spectroscopy, transmission electron microscopy, and inductively coupled plasma atomic emission spectroscopy. The results indicated that our catalyst was quite active in oxidizing the benzyl alcohols to their corresponding aldehydes in the presence of *t*-butyl hydroperoxide (TBHP). The catalyst efficiency with low catalyst loading, convenient work-up, isolation of pure products, use of inexpensive metal instead of precious metals, solvent-free condition, use of eco-friendly support, and the sustainability of catalyst up to at least 5 consecutive runs without a special drop-in activity are some of the remarkable advantages of this protocol.

1. Introduction

Excessive use of nonbiodegradable material and depletion of the planet's natural resources, as well as environmental waste problems, are convincing reasons to utilize greener sources like biopolymer-based material. Biopolymers (polynucleotides, polypeptides, and polysaccharides) are naturally occurring polymers produced by living organisms. Due to their low cost, good stabilizing capability, and green nature, biopolymers have been widely used in biotechnology, agriculture, medicine, drug delivery, catalysis, textile, and industrial purposes [1–7]. Pectin is defined as a linear polysaccharide consisting chiefly of D-galacturonic acid units linked together with *a* (1-4)-glycosidic linkages called homogalacturonan (HG) [8]. The galacturonic acid residues may be methylated, acetylated, or amidated at different degrees [9]. As is known, pectin has been used for many years in the food and beverage industry as a thickening and gelling agent and a colloidal stabilizer agent. The presence of free functional groups such as carboxyl and hydroxyl on the

---

*. *Corresponding author. Tel./Fax: +985632345192*
E-mail addresses: gbagherzade@gmail.com, and bagherzadeh@birjand.ac.ir (Gh. Bagherzade)

doi: 10.24200/sci.2021.58355.5689

surface of pectin has enabled it to be used as a matrix for the delivery of various drugs, proteins, and cells [10]. Pectin has been used as a green and eco-friendly catalyst for the synthesis of benzimidazoles [11]. Additionally, the synthesis of tetrahydro benzo[*b*]pyrans and pyrano[*c*]chromenes is also catalyzed by pectin [12]. Pectin acts as an organocatalyst and develops these reactions through green and metal-free processes. Bio-derived nanocomposites merge the properties of their constituents to produce a novel nanomaterial with increased abilities such as mechanical, electrical, and optical properties, enhanced stability, biocompatibility, and lower toxicity. Due to its intrinsic properties such as gelling properties, complexation, and large surface area, pectin has been used for the preparation of numerous composite materials with various applications in catalysis and photocatalyst [13–18]. Post-modification of bio-polymers is often used to generate new properties on their surface [19,20]. In addition, the magnetization of bio-polymers is an attractive approach because it facilitates the separation of nanocatalyst from the reaction mixture and decreases the contamination of the final product caused by the presence of catalyst [21–23]. Literature survey shows only a few examples of magnetic pectin-based nanocomposites [24,25]. Selective oxidation of alcohols to carbonyl compounds is an essential transformation in organic synthesis with a remarkable application in both the laboratory and the industry [26–28]. Typically, such modifications have been made with stoichiometric amounts of metal-based oxidizing reagents such as chromates, bromates, and permanganates [29]. These metal-based reagents produce environmental pollutants that lead to the use of catalytic-promoted oxidation of alcohols. Therefore, nowadays, catalyst-promoted oxidation of alcohols using various oxidants such as air, dioxygen, *t*-butyl hydroperoxide (TBHP), H_2O_2, and NaOCl has attracted much attention [30–35]. To increase activity and selectivity, catalysts based on noble metals such as Ru [36], Pd [37], Ag [38], and Au [39] have been developed. These noble metals are subject to some disadvantages like high cost and scarcity [40]. Thus, designing a catalyst that combines activity with selectivity at a lower price and follows green chemistry instructions is of great importance. In this paper, we would like to demonstrate a green, inexpensive and straightforward protocol for the oxidation of benzyl alcohols using TBHP as an oxidant and Fe_3O_4@Pectin∼Imidazole∼SO_3H-Cu(II) as an efficient biopolymer-based magnetic nanocatalyst under solvent-free conditions (Scheme 1).

2. Experimental

2.1. Materials and methods

All commercially available chemicals were purchased from Merck or Aldrich Company and used without further purifications. The products were characterized based on a comparison of their spectral data and physical properties with authentic samples reported in the literature. The reaction progress was monitored by TLC using Merck 0.2 mm SILG/UV254 plates. Fourier transform infrared spectroscopy (FT-IR) spectra were obtained as KBr pellets on a Nicolet system 800 beam splitter SCAL = 800 in the 400–4000 cm^{-1} spectrometers. ^{1}HNMR spectra were recorded on a Bruker DRX 250 MHz Avance spectrometer in DMSO-d_6 as solvent at ambient temperature using Tetramethylsilane (TMS) as an internal standard. The melting point of products was inquired in open capillaries with Electrothermal IA9100 melting point apparatus and is reported without correction. The crystal structure of the catalyst was analyzed on an X'Pert MPD Philips diffractometric with Cu radiation source (λ = 1.54050 Å) at 40 kV voltage and 40 mA current. The magnetic properties of the nanocatalyst were investigated using Vibrating Sample Magnetometer (VSM, BHV-55, Riken, Japan) at room temperature. The surface morphology, size, and shape of the catalyst were examined by Field Emission Scanning Electron Microscopy (FESEM, MIRA3, TESCAN, Czech Republic) equipped with an Energy Dispersive X-ray detector (EDX) to identify the chemical elements. Transmission Electron Microscopy (TEM) images were recorded using a Philips CM120 microscope. In addition, the concentration of Cu(II) in the catalyst (1) was estimated by Inductively Coupled Plasma (ICP) atomic emission spectroscopy on an OPTIMA 7300DV apparatus.

2.2. Preparation magnetic pectin (Fe_3O_4@Pectin)

First, pectin (1.0 g) was dissolved in 50 mL of distilled water and stirred for 2–3 h at room temperature to produce a white gelatine material. Then, a solution of $FeCl_3.6H_2O$ (3 g) and $FeCl_2.4H_2O$ (1 g) dissolved in 120 mL distilled water was slowly added to the premixed solution under ultrasonic irradiation. The obtained solution was then refluxed under the N_2 atmosphere at 90°C for 2 h. After that, 11 mL of 28% NH_4OH was added slowly to the resulting mixture followed by stirring under the reflux at 90°C for 1 h. The obtained black precipitate was thoroughly washed with distilled water and ethanol to remove the unreacted materials and then, was dried at room temperature to produce Fe_3O_4@Pectin.

2.3. Preparation of CPTMS-modified magnetic pectin (Fe_3O_4@Pectin∼CPTMS)

Briefly, 1.0 g of Fe_3O_4@Pectin nanoparticles were added to 10 mL dried toluene and dispersed by ultrasonic irradiation. Then, 2.5 mL of 3-

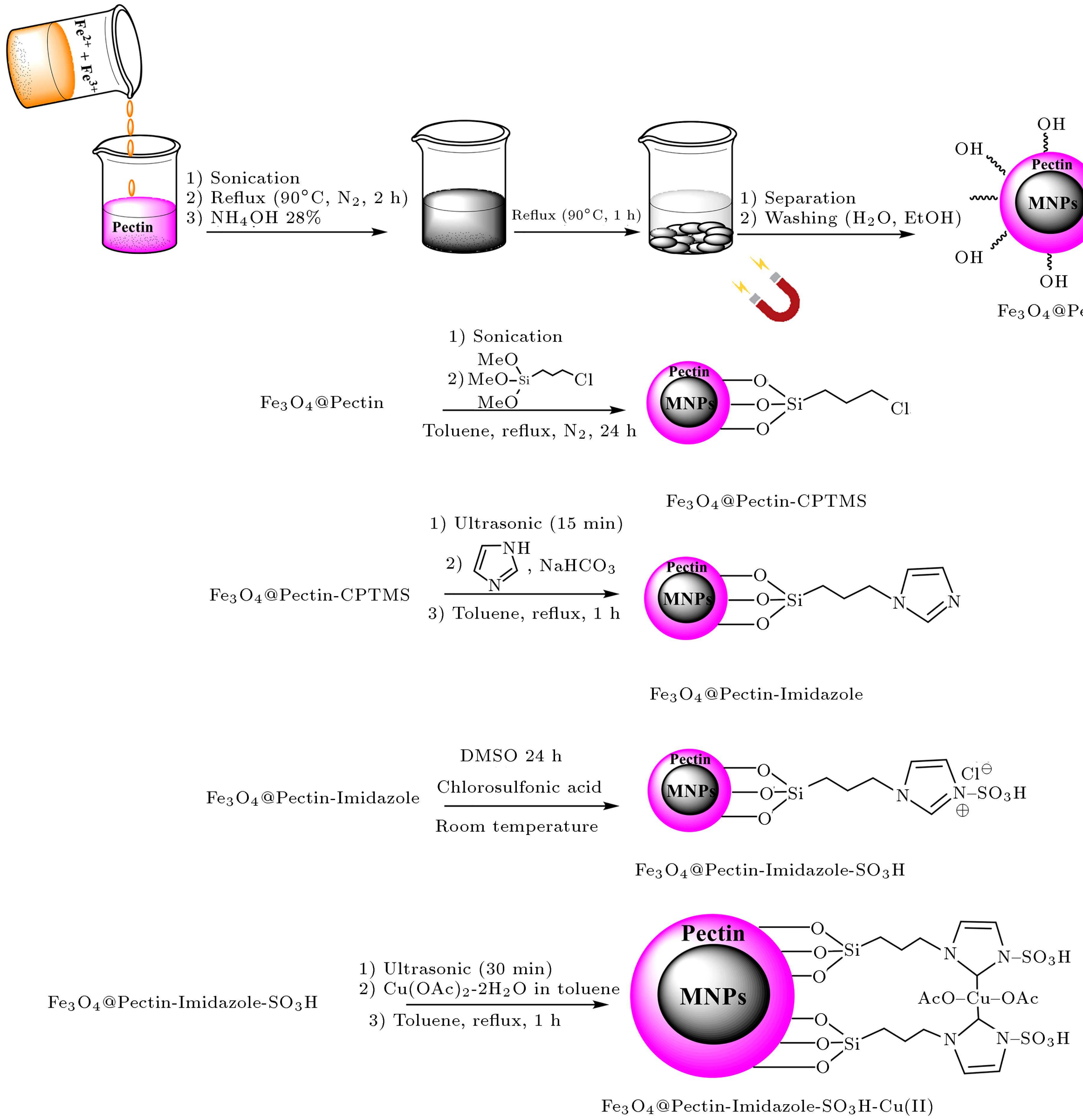

Scheme 1. General description of the synthesis of Fe_3O_4@Pectin∼Imidazole∼SO_3H-Cu(II) magnetic nanocatalyst.

chloropropyltrimethoxysilane (CPTMS) was added to the system and the mixture was stirred for 15 min, followed by further stirring under the reflux for 24 h. After washing with toluene and water, the obtained magnetic nanoparticles were separated using an external magnet and dried at room temperature to prepare the (Fe_3O_4@Pectin∼CPTMS) nanoparticles.

2.4. Preparation of imidazole-functionalized magnetic pectin (Fe_3O_4@Pectin∼Imidazole)

To prepare imidazole-functionalized magnetic pectin (Fe_3O_4@Pectin∼CPTMS-Imidazole), the Fe_3O_4@ Pectin∼CPTMS (1.9 g) nanoparticles were dispersed in dry toluene (20 mL) and sonicated for 15 min. To this solution, imidazole (0.24 g, 3.5 mmol) and sodium bicarbonate (0.672 g, 0.008 mol) were simultaneously added and the sonication was continued for 15 min. Subsequently, the mixture was refluxed for 24 h. After that, the product was separated by using an external magnet and thoroughly washed by dry diethyl ether (3 × 10 mL) to remove the unreacted substrates. Finally, the product (Fe_3O_4@Pectin∼ Imidazole) was then dried under vacuum at room temperature for 12 h.

2.5. Synthesis of sulfonated Fe_3O_4@Pectin∼Imidazole (Fe_3O_4@Pectin∼Imidazole∼SO_3H)

The synthesized Fe_3O_4@Pectin∼Imidazole (1 g) was sonicated in DMSO (30 mL) for 30 min. Chlorosulfonic acid (3 mL) was slowly added dropwise to the dispersed mixture in an ice bath and stirred for 24 h at room temperature. The solid was separated by an external magnet, washed with H_2O to reach pH 6–7, and dried at 70°C in the oven under vacuum.

2.6. Cu(II) immobilization on Fe_3O_4@Pectin∼Imidazole∼SO_3H

First, 1 g of Fe_3O_4@Pectin∼Imidazole∼SO_3H was dispersed in 10 mL dry toluene and sonicated for 30 min. To this solution, a mixture of Cu $(OAc)_2$ (0.9 g, 5 mmol) dispersed in 5 mL dry toluene was added slowly and the sonication was continued for 15 min, followed by stirring under the reflux conditions for 24 h. After that, the product was separated using an external magnet and washed with dry diethyl ether (3 × 10 mL) to remove the unreacted substrates. The resulting catalyst was dried overnight under vacuum and the final obtained material was labelled as Fe_3O_4@Pectin∼Imidazole∼SO_3H-Cu(II). General description of the preparation of Fe_3O_4@Pectin∼Imidazole∼SO_3H-Cu(II) is shown in Scheme 1.

2.7. General procedure for benzyl alcohol oxidation using Fe_3O_4@Pectin∼Imidazole∼SO_3H-Cu(II) nanocatalyst

A mixture of benzyl alcohol (1a-9a, 0.1 mL), tert-butyl hydroperoxide (TBHP, 0.2 mmol, 0.02 mL), and Fe_3O_4@Pectin∼Imidazole∼SO_3H-Cu(II) (1.5 mol%) was stirred at 40°C within an appropriate time in solvent-free conditions to facilitate the corresponding aldehyde. After completion of the reaction, as monitored by TLC [eluent: *n*-hexane: ethyl acetate: 8:2], the reaction was cooled to room temperature and the catalyst was separated using an external magnet. The residue was concentrated to result in the corresponding aldehyde (1b-9b).

3. Result and discussion

3.1. Catalyst characterization

In this work, Fe_3O_4@Pectin∼Imidazole∼SO_3H-Cu(II) catalyst was prepared in several steps. At step one, the oxygen atom in the magnetite (Fe_3O_4) attacked the pectin as a nucleophile and a C-O bond was formed by the interaction between the Fe_3O_4 and the pectin. Then, silane, copper-metal complex added to the mixture of Fe_3O_4@Pect. Fe_3O_4, Fe_3O_4@Pect, Imidazole, and Fe_3O_4@Pectin∼CPTMS-Imidazole-Cu(II) was prepared (Scheme 1). After the successful synthesis of nanocomposite (Scheme 1), the Magnetic nanocomposite was characterized using various standard physicochemical techniques such as FT-IR, powder X-Ray Diffraction analysis (XRD), TEM, Scanning Electron Microscopy (FESEM), VSM, and EDS. FT-IR spectra of:

(a) Pectin;
(b) Fe_3O_4@Pect;
(c) Fe_3O_4@Pectin∼CPTMS;
(d) Fe_3O_4@Pectin∼Imidazole, and
(e) Fe_3O_4@Pectin∼Imidazole∼SO_3H-Cu(II),

are shown in Figure 1(a)–(e), respectively. The FT-IR spectrum of pectin (Figure 1(a)) shows the stretching vibrations of the O-H group at 3200–3450 cm^{-1} and the stretching vibrations of the C=O, C-O group at around 1710 cm^{-1} and 1120 cm^{-1}. As shown in the FT-IR spectrum of Fe_3O_4@Pect (Figure 1(b)), the stretching vibrations Fe-O and O-H at 577 cm^{-1} and 3420 cm^{-1} confirmed the formation of Fe_3O_4 nanoparticles. Also, in the FT-IR spectrum of Fe_3O_4@Pectin∼CPTMS (Figure 1(c)), a new sharp peak at 1155 cm^{-1} was assigned to the stretching vibration of Si–O. Immobilization of imidazole on the Fe_3O_4@Pectin∼CPTMS was confirmed by the peak that appeared at 1641 cm^{-1} (Figure 1(d)), indicating that the imidazole was supported on the Fe_3O_4@Pectin∼CPTMS. Furthermore, the complexation of copper ions to imidazole causes the imine bond absorption at 1641 cm^{-1} to lower wavenumbers 1616 cm^{-1} by about 25 cm^{-1}, indicating

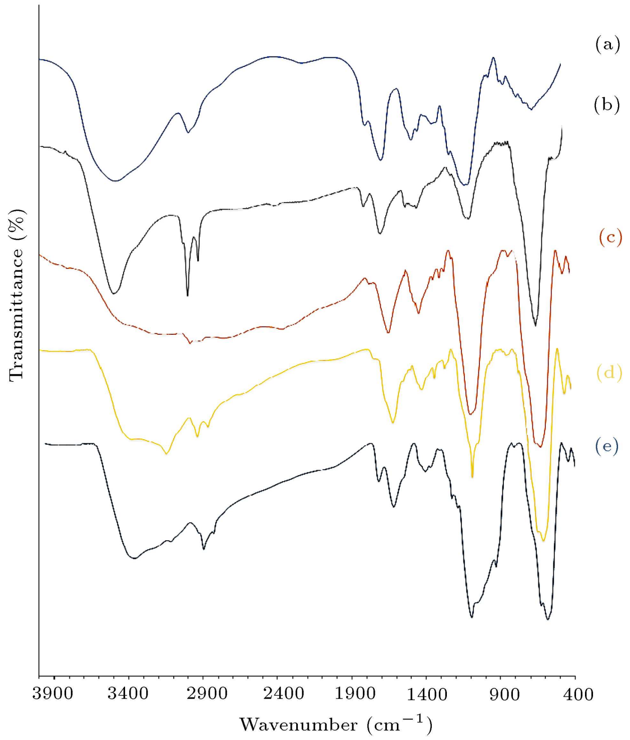

Figure 1. FT-IR spectrum of (a) Pectin, (b) Fe_3O_4@Pectin, (c) Fe_3O_4@Pectin∼CPTMS, (d) Fe_3O_4@Pectin∼Imidazole, and (e) Fe_3O_4@Pectin∼Imidazole∼SO_3H-Cu(II).

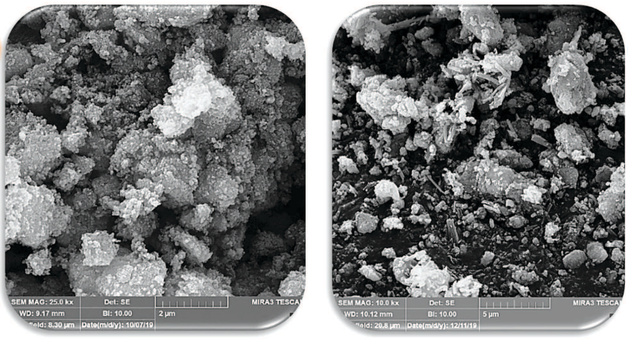

(a) (b)

Figure 2. FESEM image of (a) Fe_3O_4 and (b) Fe_3O_4@Pectin~Imidazole~SO_3H-Cu(II).

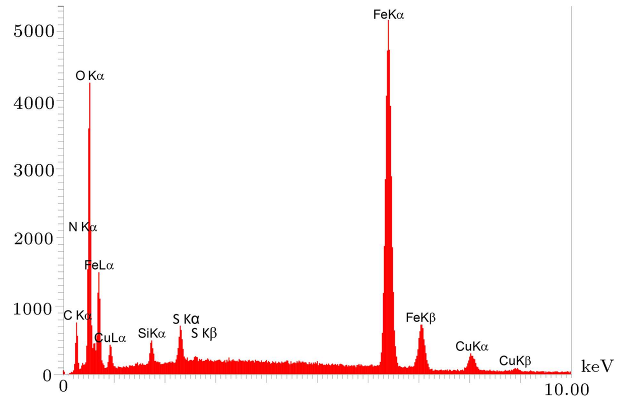

Figure 3. EDX spectra of Fe_3O_4@Pectin~Imidazole~SO_3H-Cu(II) nanocomposites.

the participation of azomethine nitrogen in bonding with metal ion and confirming the coordination of ν(C=V) stretch to the metal via a nitrogen atom. The main absorption bands including (Fe–O), (Si–O), (C-N), and (C=N) in the FT-IR spectrum of Fe_3O_4@Pectin~Imidazole~SO_3H-Cu(II) represent the successful functionalization of Fe_3O_4@Pect nanoparticles with imidazole and finally, its complexion with Cu(II) (Figure 1(e)).

FESEM images were used for further research of the surface morphology of the prepared catalyst. The FESEM image is shown in Figure 2. Particle size and the morphology FESEM micrographs indicated that Fe_3O_4@Pectin~Imidazole~SO_3H-Cu(II) nanocomposites were almost aggregated spheroidal-shaped particles in size from 29 to 35 nm, showing good agreement with the calculated result from the Debye-Scherrer equation. Some aggregation occurs due to the magnetic property of nanoparticles.

The composition and distribution of individual components in the Fe_3O_4@Pectin~Imidazole~SO_3H-Cu(II) nanocomposites were studied using EDX. The results depicted well-defined peaks of Cu, Fe, Si, C, N, and O (Figure 3).

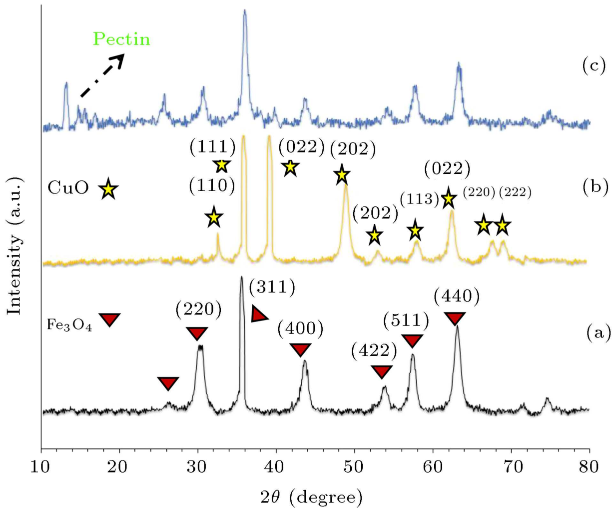

Figure 4. XRD pattern of (a) Fe_3O_4, (b) CuO, and (c) Fe_3O_4@Pectin~Imidazole~SO_3H-Cu(II).

The crystalline structures of the Fe_3O_4 particles, CuO, and Fe_3O_4@Pectin~Imidazole~SO_3H-Cu(II) were determined by powder XRD. As shown in Figure 4(a), it can be seen that the characteristic broad diffraction peaks shown in wide-angle XRD patterns can be indexed to the cubic spinel magnetite Fe_3O_4 crystal structure, which shows diffraction peaks; the patterns indicate a crystallized structure at 2θ: 30.3°, 35.8°, 43.6°, 54.8°, 57.3°, and 63.2°, which are assigned to (220), (311), (400), (422), (511), and (440) [41]. Also, the XRD pattern of the CuO (Figure 4(b)) shows the peaks at 2θ = 32.07°, 35.47°, 35.82°, 48.72°, 52.97°, 58.02°, 62.47°, 67.87°, and 69.32° corresponding to the (110), (111), (022), (202), (202), (113), (022), (220), and (222) crystallographic phases in XRD pattern that are related to CuO. The low-angle XRD pattern of the Fe_3O_4@Pectin~Imidazole~SO_3H-Cu(II) was also investigated, as depicted in Figure 4(b). The XRD pattern of Fe_3O_4@Pectin~Imidazole~SO_3H-Cu(II) prepared by the Stöber process shows pronounced diffusion peaks from 12 to 14 that appeared because of pectin (Figure 4(c)). The XRD patterns of Fe_3O_4 and Cu(II) immobilized on Fe_3O_4@Pectin~Imidazole~SO_3H-Cu(II) show characteristic peaks whose relative intensities match well with the reported XRD of Fe_3O_4 magnetite. On the other hand, these results indicate that the crystal structure of Fe_3O_4@Pectin~Imidazole~SO_3H-Cu(II) nanoparticles does not vary after modification with Imidazole, which means that the copper sites are in their Cu(II) status. These explanations and results imply that the spinel structure of Fe_3O_4 and Cu(II) has been retained during the process of catalyst preparation.

The values of the magnetization saturation (M_s) for Fe_3O_4 and Fe_3O_4@Pectin~Imidazole~SO_3H-Cu(II) were calculated to be 62.91 and 53.00 emu/g, respectively (Figure 5). This catalyst demonstrated

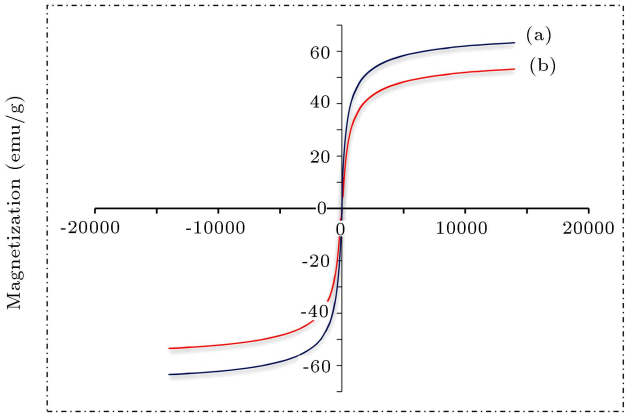

Figure 5. Magnetization curves of Fe$_3$O$_4$ (a) and Fe$_3$O$_4$@Pectin$\sim$Imidazole$\sim$SO$_3$H-Cu(II) (b) at room temperature..

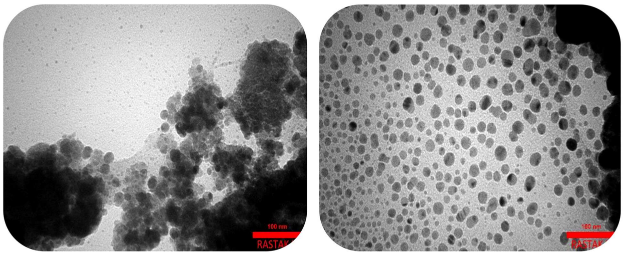

Figure 6. Transmission electron microscope image of the Fe$_3$O$_4$@Pectin$\sim$Imidazole$\sim$SO$_3$H-Cu(II).

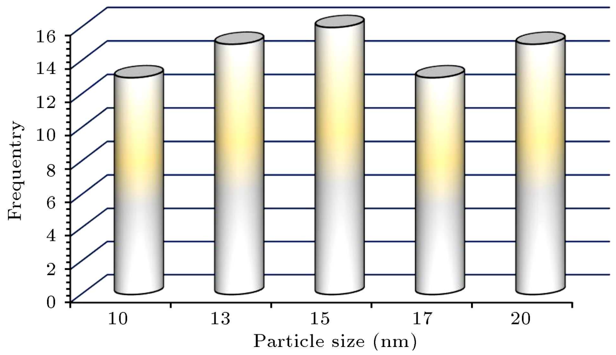

Figure 7. Particle size distribution histogram of Fe$_3$O$_4$@Pectin$\sim$Imidazole$\sim$SO$_3$H-Cu(II).

that the Fe$_3$O$_4$@Pectin$\sim$Imidazole$\sim$SO$_3$H-Cu(II) was superparamagnetic. Compared with the uncoated Fe$_3$O$_4$, the saturation magnetization of the Fe$_3$O$_4$ and Fe$_3$O$_4$@Pectin$\sim$Imidazole$\sim$SO$_3$H-Cu(II) decreased because the diamagnetic contribution of the thick pectin and organic matter resulted in a low mass deduction of Fe$_3$O$_4$ magnetic substance.

The structure of Fe$_3$O$_4$@Pectin$\sim$Imidazole$\sim$SO$_3$H-Cu(II) was studied by TEM (Figure 6). These images represent a suitable tool for determining the size and structure of particles. The TEM images and histogram Fe$_3$O$_4$ @Pectin$\sim$Imidazole$\sim$SO$_3$H-Cu(II) show the small particles of 16–28 nm (Figure 7).

3.2. Oxidation of benzyl alcohols

The catalytic activity of Fe$_3$O$_4$@Pectin$\sim$Imidazole$\sim$SO$_3$H-Cu(II) was initially investigated in a standard reaction using benzyl alcohol (1a, 1 mmol) and the effects of variation in reaction parameters such as solvent (Table 1, entries 1–4), catalyst loading (Table 1, entries 5 and 6), TBHP (Table 1, entries 7 and 8), temperature (Table 1, entries 9–12), and time (Table 1, entries 13–16) were studied to develop the general reaction conditions. The results are summarized in Table 1. In the first experiment, the effect of various solvents was explored while the time, catalyst loading, and ratio of oxidants were constant (entries 1–4). As can be seen, the best result in the case of yield 95% was obtained under the solvent-free conditions (Table 1, entry 4), although the reaction could even be accomplished in the other solvents. After that, the effect of catalyst loading was evaluated under the solvent-free condition (Table 1, entries 5–7). The results demonstrate that an increase in the catalyst loading from 1 mol% to 2 mol% enhances the yield of 95% of the product. However, with 3 mol% catalyst loading, an identical yield of 90% was achieved, indicating that 2 mol% was the optimum amount of catalyst loading (Table 1, entry 4). In addition, the effect of the TBHP ratio was investigated and the results demonstrated that with 1 mmol TBHP (Table 1, entry 7), the corresponding product was produced at a lower yield of 85% than 2 mmol TBHP, while using 3 mmol TBHP (Table 1, entry 8) without improvement in yield 90% of the product (1b) was observed. Then, the model reaction was carried out under solvent-free conditions at room temperature, 40–70°C (entries 9–12). The product yield was increased up to 40°C and was decreased significantly to 60°C. Temperature as an effective parameter may improve the yield of the product. Therefore, the reactions were conducted at different temperatures including room temperature 40, 60, and 70°C (Table 1, entries 10–13).

The reduction in the product yield could be due to the decomposition of TBHP to molecular water and tert-butanol in the presence of Fe$_3$O$_4$@Pectin$\sim$Imidazole$\sim$SO$_3$H-Cu(II) at evaluated temperatures. As a result, 40°C was selected as the optimized reaction temperature. To investigate time, different reaction times (Table 1, entries 13–16) were examined at the fixed parameters (40°C, solvent-free and 2 mmol of TBHP). Based on the results, longer reaction times enhanced the yield of 85% of reaction and the highest yield of 95% was obtained when the reaction was stirred for 60 min (Table 1, entry 4). Therefore, the optimum reaction condition for the oxidation of benzyl alcohols was determined as a reaction with benzyl alcohols (1a-15a, 1 mmol) at 40°C in the solvent-free condition using TBHP (2 mmol) as the oxidant, which is depicted in Table 1, entry 4. In addition to TBHP, oxidation of benzyl alcohol (1b) was

Table 1. Optimization of reaction conditions for the oxidation of benzyl alcohols (1a–9a) using benzyl alcohol (3a); a model reaction substrate.[a]

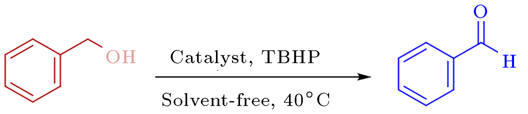

1a **1b**

Entry	Solvent	Temp. (°C)	Time (min)	Catalyst (mol%)	TBHP (mmol)	Yield (%)[b]
1	EtOH	80	60	2	2	55
2	H_2O	90	60	2	2	60
3	CH_3CN	70	60	2	2	80
4	Solvent-free	40	60	2	2	95
5	Solvent-free	40	60	1	2	75
6	Solvent-free	40	60	3	2	90
7	Solvent-free	40	60	2	1	85
8	Solvent-free	40	60	2	3	90
9	Solvent-free	r.t.	60	2	2	65
10	Solvent-free	50	60	2	2	95
11	Solvent-free	60	60	2	2	90
12	Solvent-free	70	60	2	2	85
13	Solvent-free	40	20	2	2	80
14	Solvent-free	40	40	2	2	90
15	Solvent-free	40	80	2	2	93
16	Solvent-free	40	100	2	2	85

[a]: Reaction conditions specified in the table subtitle: The reactions were performed with benzyl alcohol (1a, 1 mmol) and different values of *tert*-butyl hydroperoxide (TBHP) and 4 mL of each solvent.

[b]: Isolated yield.

Table 2. Screening the nature of oxidants[a].

Entry	Oxidant	Time (min)	Yield[b] (%)
1	H_2O_2	75	80
2	$NaIO_4$	75	55
3	TBHP	75	95

[a]: Reaction conditions: Benzyl alcohol (1 mmol), oxidant (2 mmol), catalyst (2 mol%), 40°C.

[b]: Yields of product isolated.

carried out using other oxidants like H_2O_2 and $NaIO_4$ and the results confirmed the superiority of TBHP (Table 2).

With the optimized reaction conditions in hand, the scope and generality of the alcohol oxidation reaction were extended. The obtained results are presented in Table 1. A lot of structurally diverse primary and secondary benzyl alcohols were oxidized by Fe_3O_4@Pectin~Imidazole~SO_3H-Cu(II) with TBHP in solvent-free conditions, producing excellent yields (75–97%) of aromatic aldehydes (entries 1–11, Table 3)/ketones (entries 12–15, Table 3). Various benzyl alcohols with electron-donating and electron-withdrawing groups in ortho-/meta-/and para positions of the benzene ring were smoothly converted into corresponding aromatic aldehydes in good to excellent yields under optimized reaction conditions, regardless of the electronic nature and position of the substituent. Secondary alcohols were effectively converted into corresponding ketones by UoB-5 with TBHP. Moreover, cinnamyl alcohol was selectively oxidized to cinnamaldehyde without any by-products in good yield (entry 14, 75%). To evaluate the performance of the Fe_3O_4@Pectin~Imidazole~SO_3H-Cu(II) catalyst in the alcohol oxidation reaction, the model reaction was induced within 7 h under the optimization condition; in addition, this is nanocatalyst selectivity and the product stops at the aldehyde phase. No other by-products including carboxylic acid are not formed. This is an indication of the selectivity of Fe_3O_4@Pectin~Imidazole~SO_3H-Cu(II) nanocatalyst.

The proposed reaction mechanism for the oxidation of benzyl alcohols (1a-9a) using TBHP in the presence of Fe_3O_4@Pectin~Imidazole~SO_3H-Cu(II) based on the available literature [42–44] is shown in Scheme 2. Decomposition of the *t*-BuOOH on the surface of Fe_3O_4@Pectin~CPTMS-Imidazole-Cu(II) leads to the formation of *t*-BuOO$^\bullet$ radical species and reduction of Cu(II) to Cu(I). In addition, the decomposition of *t*-BuOOH on the surface of Cu(I) generates *t*-BuO$^\bullet$

Table 3. Oxidation of various alcohols using TBHP and Fe_3O_4@Pectin~Imidazole~SO_3H-Cu(II) magnetic nanocatalyst[a].

Entry	Substrate (1a–15a)	Product (2b–15b)	Time (min)	Yield[b] (%)
1	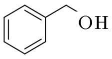	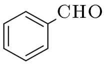	60	95
2	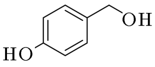	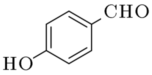	60	95
3	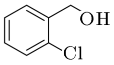	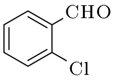	45	90
4	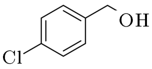	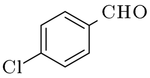	45	92
5	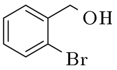	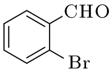	60	88
6	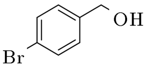	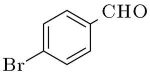	60	82
7	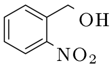	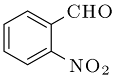	75	80
8	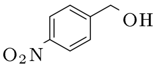	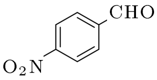	75	85
9	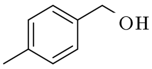	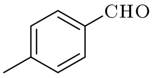	60	95
10	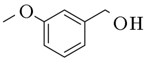	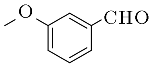	50	85
11	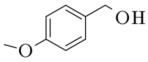	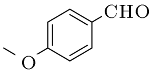	50	95
12	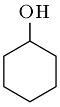	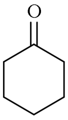	90	80
13	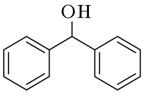	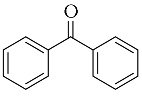	50	95
14	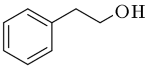	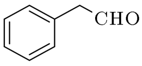	50	75
15	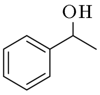	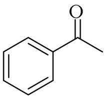	50	97

[a]: Reaction conditions: The reactions performed with benzyl alcohols (1a–15a, 1 mmol) and TBHP (2 mmol) in solvent-free conditions at 40°C.

[b]: Isolated yield.

Table 4. Comparison of this method with some of the previously reported methods for benzyl alcohol reaction.

Entry	**Catalyst (mg or mol%)**	**Solvent**	**Oxidant (mL)**	**Temp (°C)**	**Time (h)**	**Yield (%)**	**Reference**
1	$LaCrO_3$ (10 mol%)	Solvent-free	TBHP	90	2:30	79	[35]
2	Cu@imine-nanoSiO_2 (0.25 mol%)	CH_3CN	TBHP	50	5	67	[42]
3	g-C_3N_4@CuO (3 mg)	H_2O	TBHP	r.t	5	93	[44]
4	Fe_3O_4@BNPs-CPTMS-Chitosan-Pd(0) (2.8 mol%)	EtOH	H_2O_2	50	4	70	[45]
5	Dicopper(II)-tetra carboxylates (0.5 mol%)	MeOH	TBHP	65	3	82	[46]
6	SBA-15Co-Si (100 mg)	*n*-Hexane	TBHP	70	15	57	[47]
7	Silica-Supported $CuCo_2O_4$ (21.6 mg)	EtOH	TEMPO	100	8	94	[48]
8	**Fe_3O_4@Pectin~Imidazole~SO_3H-Cu(II)** **(2 mol%: 8 mg)**	**Solvent-free**	**TBHP**	**40**	**1**	**95**	**This work**

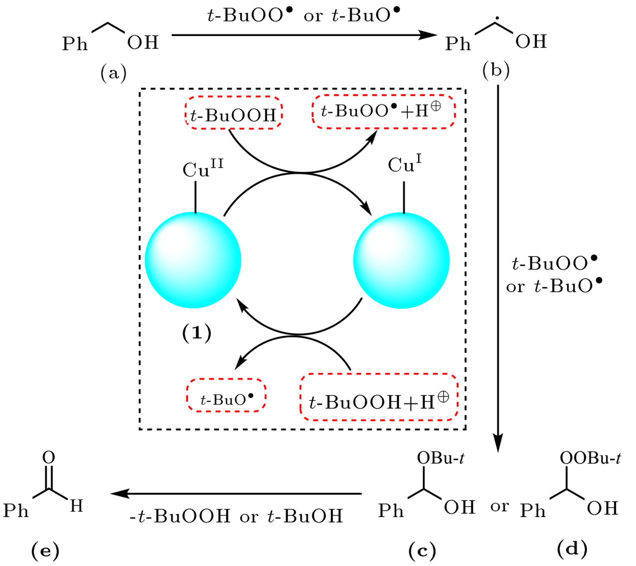

Scheme 2. Plausible mechanism for the oxidation of benzyl alcohols (1a-15a) using TBHP in the presence of Fe_3O_4@Pectin~Imidazole~SO_3H-Cu(II).

species. Next, *t*-BuOO• and *t*-BuO• radical species underwent hydrogen abstraction of the substrate (a) to produce intermediate (b). The reaction of intermediate (b) with *t*-BuOO• and t-BuO• results in (c) and (d), ultimately producing the corresponding aldehyde (e) through elimination of *t*-BuOOH and *t*-BuOH.

To demonstrate the efficiency of the present method in the oxidation of benzyl alcohols (1a-15a) to aldehydes (1b-15b), the obtained results for the oxidation of benzyl alcohol (1a) were compared with some of the recently reported works (Table 4). The results indicate that this method is superior to some of the previously reported methods in catalyst loading, solvent, oxidant ratio, temperature, reaction time, and yield.

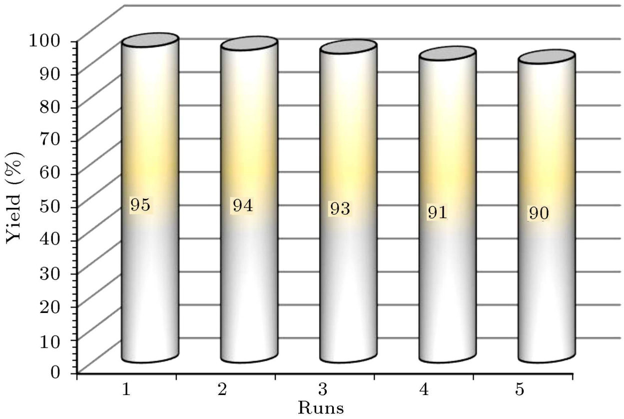

Figure 8. Recycling of Fe_3O_4@Pectin~Imidazole~SO_3H-Cu(II) in the oxidation of benzyl alcohols using 1a as a model substrate.

Recyclability and ease of separation from the reaction mixture are important to be considered for any heterogeneous catalyst. Therefore, the reusability of Fe_3O_4@Pectin~Imidazole~SO_3H-Cu(II) was explored for 1a as a model substrate. After completing the reaction, the catalyst was separated using an external magnet and washed thoroughly with water (3 × 10 mL) and ethanol (2 × 10 mL). Finally, the catalyst was dried in an oven at 60°C for 1 h. Up to five successive runs, the efficiency of the recycled catalyst was examined and its performance remained almost the same with the fresh catalyst (Figure 8).

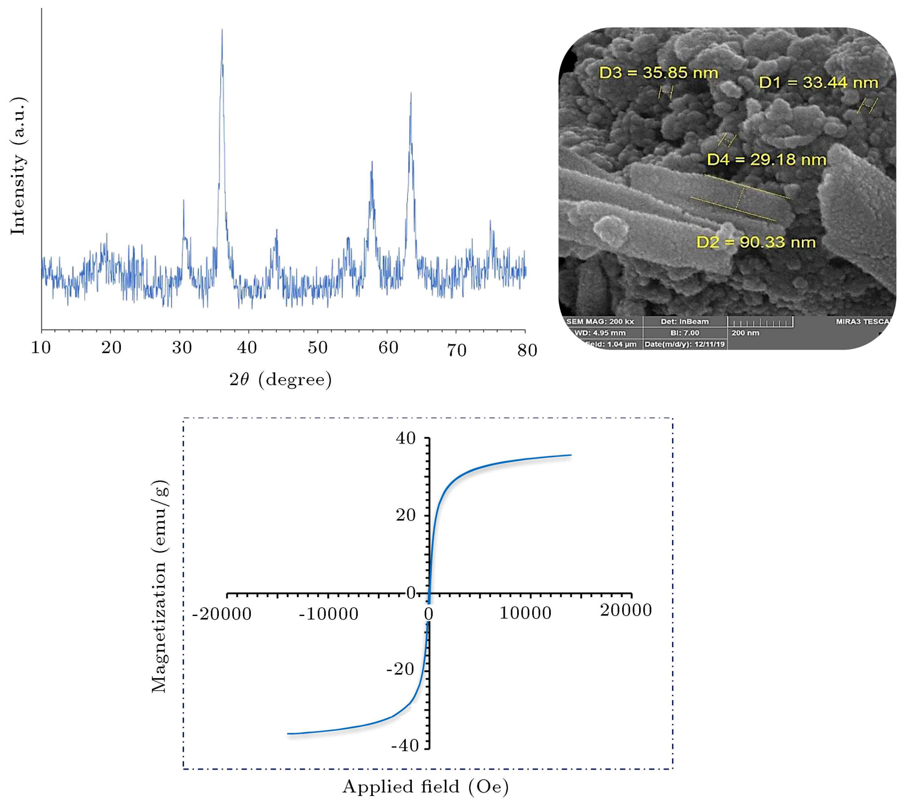

Figure 9. FESEM, VSM, and XRD analyses of Fe_3O_4@Pectin~Imidazole~SO_3H-Cu(II) after five times recycling.

Due to the magnetic properties of the catalyst after the first use of the product catalyst, it is simply extracted by ethyl acetate. In contrast, the catalyst remains at the aqueous phase. The catalyst exhibited good performance after four times of recycling. FE-SEM, VSM, and XRD of the catalyst after five times reuse showed that the structure and morphology of the catalyst remained unchanged during the recycling process (Figure 9).

4. Conclusion

In conclusion, due to the presence of open metal sites and the nature of the imidazole, it was used as an excellent two-factor heterogeneous catalyst for an alcohol oxidation reaction. Besides achieving high selectivity and activity to the target products, the heterogeneous nature of the catalyst was provided by the preservation of its structural integrity during alcohol oxidation reaction. The Fe_3O_4@Pectin~Imidazole~SO_3H-Cu(II) catalyst was used as an efficient and recyclable magnetic nanocatalyst for the oxidation of benzyl alcohols to aldehydes using t-butyl hydroperoxide (TBHP) as the oxidant without the oxidant. The reported results confirmed that this method was for oxidation of electron-bearing benzyl alcohols (such as 4-OH and 4-Me) and electron-withdrawing groups (such as 4-NO_2, 3-NO_2, 4-Cl, 2-Cl, 4-Br, and 2-Br) on the benzene ring. Mild conditions, short reaction time, green nature catalyst, production of small wastes, use of low catalyst load, and at least 5 times reusability are some of the significant advantages of this work. Fe_3O_4@Pectin~Imidazole~SO_3H-Cu(II) is an excellent candidate as a more economically favorable and environmentally friendly alternative to conventional catalysts. Also, we expect the approach of this work to be viable for the construction of many more interesting and practical two-factor catalysts like this for green organic synthesis.

Acknowledgments

We gratefully acknowledge the financial support of the research Council of the University of Birjand.

References

1. Bakherad, M., Keivanloo, A., Amin, A.H., et al. "Silica-anchored Cu(I) aminothiophenol complex: An efficient heterogeneous catalyst for synthesis of 1, 4-disubstituted 1, 2, 3-triazoles in water", *Iranian Journal of Catalysis*, **8**(3), pp. 179–187 (2018).
2. Ghamari Kargar, P., Aryanejad, S., and Bagherzade, G. "Simple synthesis of the novel Cu-MOF catalysts for the selective alcohol oxidation and the oxidative cross-coupling of amines and alcohols", *Applied Organometallic Chemistry.*, **34**(12), p. e5965 (2020).

3. Khashei Siuki, H., Bagherzade, G., and Ghamari Kargar, P. "A green method for synthesizing nickel nanoparticles supported by magnetized pectin: Applied as a catalyst for aldehyde synthesis as a precursor in xanthan synthesis", *Chemistry Select*, **5**(43), pp. 13537–13544 (2020).
4. Wathoni, N., Nguyen, A.N., Rusdin, A., et al. "Enteric-coated strategies in colorectal cancer nanoparticle drug delivery system", *Drug Des. Devel Ther.*, **14**, p. 4387 (2020).
5. Pettignano, A., Aguilera, D.A., Tanchoux, N., et al. "Alginate: A versatile biopolymer for functional advanced materials for catalysis", *Stud Surf Sci Catal.*, **178**, pp. 357–375 (2019).
6. Ghamari Kargar, P., Len, C., and Luque, R. "Cu/cellulose-modified magnetite nanocomposites as a highly active and selective catalyst for ultrasound-promoted aqueous O-arylation Ullmann and sp-sp2 Sonogashira cross-coupling reactions", *Sustainable Chemistry and Pharmacy*, **27**, 100672 (2022).
7. Ghamari kargar, P., Noorian, M., Chamani, E., et al. "Synthesis, characterization and cytotoxicity evaluation of a novel magnetic nanocomposite with iron oxide deposited on cellulose nanofibers with nickel (Fe_3O_4@NFC@ONSM-Ni)", *RSC Adv.*, **11**, pp. 17413–17430 (2021).
8. Marcon, M.V., Vriesmann, L.C., Wosiacki, G., et al. "Pectins from apple pomace", *Polímeros.*, **15**(2), pp. 127–129 (2005).
9. Cervenka, L., Zachova, I., Minarikova, P., et al. "Effect of pH and water activity on the growth of Arcobacter sp. in culture", *Czech J. Food Sci.*, **15**(2), p. 112 (2003).
10. Sriamornsak, P. "Chemistry of pectin and its pharmaceutical uses: A review", *SUSTJ.*, **3**(1–2), pp. 206–228 (2003).
11. Khashei Siuki, H., Ghamari Kargar, P., and Bagherzade, G. "New acetamidine Cu (II) Schiff base complex supported on magnetic nanoparticles pectin for the synthesis of triazoles using click chemistry", *Scientific Reports*, **12**(1), pp. 1–17 (2022).
12. Kangani, M., Hazeri, N., and Maghsoodlou, M.T. "A mild and environmentally benign synthesis of tetrahydrobenzo[*b*] pyrans and pyrano[*c*] chromenes using pectin as a green and biodegradable catalyst", *J Chin Chem Soc.*, **63**(11), pp. 896–901 (2016).
13. Nabi, S.A., Shahadat, M., Bushra, R., et al. "Development of composite ion-exchange adsorbent for pollutants removal from environmental wastes", *Chem. Eng. J.*, **165**(2), pp. 405–412 (2010).
14. Pathania, D., Sarita, S., and Rathore, B.S. "Synthesis, characterization and photocatalytic application of bovine serum albumin capped cadmium sulphide nanopartilces", *Chalcogenide Lett.*, **8**(6), pp. 396–404 (2011).
15. Baran, T. "Bio-synthesis and structural characterization of highly stable silver nanoparticles decorated on a sustainable bio-composite for catalytic reduction of nitroarenes", *J. Mol. Struct.*, **1182**, pp. 213–218 (2019).
16. Ghamari Kargar, P., Ravanjamjah, A., and Bagherzade, G. "A novel water-dispersible and magnetically recyclable nickel nanoparticles for the one-pot reduction-Schiff base condensation of nitroarenes in pure water", *J. Chin. Chem. Soc.*, **68**, pp. 1916–1933 (2021).
17. Baran, T. "Pd(0) nanocatalyst stabilized on a novel agar/pectin composite and its catalytic activity in the synthesis of biphenyl compounds by Suzuki-Miyaura cross coupling reaction and reduction of o-nitroaniline", *Carbohydr. Polym.*, **195**, pp. 45–52 (2018).
18. Khazaei, A., Rahmati, S., Hekmatian, Z., et al. "A green approach for the synthesis of palladium nanoparticles supported on pectin: Application as a catalyst for solvent-free Mizoroki-Heck reaction", *J. Mol. Catal. A Chem.*, **372**, pp. 160–166 (2013).
19. Wang, X., Hu, P., Xue, F., et al. "Cellulose-supported N-heterocyclic carbene-palladium catalyst: Synthesis and its applications in the Suzuki cross-coupling reaction", *Carbohydr. Polym.*, **114**, pp. 476–483 (2014).
20. Rostamnia, S., Doustkhah, E., Baghban, A., et al. "Seaweed-derived κ-carrageenan: Modified κ-carrageenan as a recyclable green catalyst in the multicomponent synthesis of aminophosphonates and polyhydroquinolines", *J. Appl. Polym. Sci.*, **133**(11), p. 43190 (2016).
21. Ghamari Kargar, P., Bagherzade, G., and Eshghi, H. "Novel biocompatible core/shell Fe_3O_4@NFC@Co (ii) as a new catalyst in a multicomponent reaction: An efficient and sustainable methodology and novel reusable material for one-pot synthesis of 4H-pyran and pyranopyrazole in aqueous media", *RSC Adv.*, **10**(61), pp. 37086–37097 (2020).
22. Ghamari Kargar, P., Bagherzade, G., and Eshghi, H. "Introduction of a trinuclear manganese (iii) catalyst on the surface of magnetic cellulose as an eco-benign, efficient and reusable novel heterogeneous catalyst for the multi-component synthesis of new derivatives of xanthene", *RSC Adv.*, **11**(8), pp. 4339–4355 (2021).
23. Ghamari Kargar, P., Bagherzade, G., and Eshghi, H. "Design and synthesis of magnetic Fe_3O_4@NFC-ImSalophCu nanocatalyst based on cellulose nanofibers as a new and highly efficient, reusable, stable and green catalyst for the synthesis of 1, 2, 3-triazoles", *RSC Adv.*, **10**(54), pp. 32927–32937 (2020).
24. Doustkhah, E., Heidarizadeh, M., Rostamnia, S., et al. "Copper immobilization on carboxylic acid-rich Fe_3O_4-Pectin: Cu^{2+}@ Fe_3O_4-Pectin a superparamagnetic nanobiopolymer source for click reaction", *Mater. Lett.*, **216**, pp. 139–143 (2018).

25. Gong, J.L., Wang, X.Y., Zeng, G.M., et al. "Copper (II) removal by pectin—iron oxide magnetic nanocomposite adsorbent", *Chem. Eng. Sci.*, **185**, pp. 100–107 (2012).

26. Ma, C.Y., Dou, B.J., Li, J.J., et al. "Catalytic oxidation of benzyl alcohol on Au or Au-Pd nanoparticles confined in mesoporous silica", *Appl. Catal. B.*, **92**(1–2), pp. 202–208 (2009).

27. Zhan, G., Huang, J., Du, M., et al. "Liquid phase oxidation of benzyl alcohol to benzaldehyde with novel uncalcined bioreduction Au catalysts: high activity and durability", *Chem. Eng. J.*, **187**, pp. 232–238 (2012).

28. Palermo, V., Villabrille, P.I., Vazquez, P.G., et al. "Role of vanadium and pyridine in heteropolycompounds for selective oxidation of alcohols with hydrogen peroxide", *J. Chem. Sci.*, **125**(6), pp. 1375–1383 (2013).

29. Holum, J.R. "Study of the chromium (VI) oxide-pyridine complex", *J. Org. Chem.*, **26**(12), pp. 4814–4816 (1961).

30. Renuka, M.K. and Gayathri, V. "A polymer supported Cu(II) catalyst for oxidative amidation of benzyl alcohol and substituted amines in TBHP/H_2O", *Catal. Commun.*, **104**, pp. 71–77 (2018).

31. Ghamari Kargar, P. and Bagherzade, G. "Robust, highly active, and stable supported Co(ii) nanoparticles on magnetic cellulose nanofiber-functionalized for the multi-component reactions of piperidines and alcohol oxidation", *RSC Adv.*, **11**, pp. 23192–23206 (2021).

32. Brink, G.J., Arends, I.W., and Sheldon, R.A. "Green, catalytic oxidation of alcohols in water", *Sci.*, **287**(5458), pp. 1636–1639 (2000).

33. Nasrollahzadeh, M., Bagherzadeh, M., and Karimi, H. "Preparation, characterization and catalytic activity of $CoFe_2O_4$ nanoparticles as a magnetically recoverable catalyst for selective oxidation of benzyl alcohol to benzaldehyde and reduction of organic dyes", *J. Colloid Interface Sci.*, **465**, pp. 271–278 (2016).

34. Tamizhdurai, P., Sakthinathan, S., Krishnan, P.S., et al. "Catalytic activity of ratio-dependent SBA-15 supported zirconia catalysts for highly selective oxidation of benzyl alcohol to benzaldehyde and environmental pollutant heavy metal ions detection", *J. Mol. Struct.*, **1176**, pp. 650–661 (2019).

35. Singh, S.J. and Jayaram, R.V. "Oxidation of alcohols to aldehydes and ketones using TBHP as an oxidant over $LaMO_3$ (M=Cr, Mn, Co, Ni, Fe) perovskites", *Synth. Commun.*, **42**(3), pp. 299–308 (2018).

36. Fukahori, S., Morikawa, M., and Ninomiya, J.I. "Preparation of ruthenium-containing sheet composites using a papermaking technique for selective oxidation of alcohol", *Chem. Eng. Sci.*, **157**(2–3), pp. 311–315 (2010).

37. Villa, A., Wang, D., Dimitratos, N., et al. "Pd on carbon nanotubes for liquid phase alcohol oxidation", *Catal. Today.*, **150**(1–2), pp. 8–15 (2010).

38. Yamamoto, R., Sawayama, Y.S., Shibahara, H., et al. "Promoted partial oxidation activity of supported Ag catalysts in the gas-phase catalytic oxidation of benzyl alcohol", *J. Catal.*, **234**(2), pp. 308–317 (2005).

39. Choudhary, V.R., Dhar, A., Jana, P., et al. "A green process for chlorine-free benzaldehyde from the solvent-free oxidation of benzyl alcohol with molecular oxygen over a supported nano-size gold catalyst", *Green Chem.*, **7**(11), pp. 768–770 (2005).

40. Bullock, R.M."Reaction: earth-abundant metal catalysts for energy conversions", *Chem.*, **2**(4), pp. 444–446 (2017).

41. Torii, H., Nakadai, M., Ishihara, K., et al. "Asymmetric direct aldol reaction assisted by water and a proline-derived tetrazole catalyst", *Angew. Chem., Int. Ed. Engl.*, **43**(15), pp. 1983–1986 (2004).

42. Gogoi, N., Begum, T., Dutta, S., et al. "Rice husk derived nanosilica supported Cu(II) complex: an efficient heterogeneous catalyst for oxidation of alcohols using TBHP", *RSC Adv.*, **5**(115), pp. 95344–95352 (2015).

43. (a) Tan, J., Zheng, T.Y., Yu, Y.Q. and Xu, K. "TBHP-promoted direct oxidation reaction of benzylic C_{sp^3}-H bonds to ketones", *RSC Adv.*, **7**, pp. 15176–15180 (2017).
(b) Bagherzade, G., Khashei Siuki, H., and Ghamari Kargar, P. "Use of pectin as a suitable substrate for catalyst synthesis Fe3O4@ Pectin@ Ni(II) and its application in oxidation reaction", *Medbiotech Journal*, **5**(02), pp. 1–8 (2021).

44. Rahman, T., Borah, G., and Gogoi, P.K. "Hybrid composite of CuO with g-C_3N_4 as a photoactive catalyst: an efficient approach for the oxidation of alcohols", *J. Chem. Sci.*, **131**(1), pp. 1–9 (2019).

45. Khodamorady, M. and Bahrami, K. "Fe_3O_4@BNPs-CPTMS-Chitosan-Pd (0) as an efficient and stable heterogeneous magnetic nanocatalyst for the chemoselective oxidation of alcohols and homoselective synthesis of 5-subestituted 1H-tetrazoles", *Chemistry Select.*, **4**(28), pp. 8183–8194 (2019).

46. Sarmah, P., Das, B.K., and Phukan, P. "Novel dicopper (II)-tetracarboxylates as catalysts for selective oxidation of benzyl alcohols with aqueous TBHP", *Catal. Commun.*, **11**(10), pp. 932–935 (2010).

47. Baskaran, T., Kumaravel, R., Christopher, J., et al. "Synthesis and heterogenization of siloxane functionalized cobalt complex: Potential catalyst for oxidation of alcohols", *Catal. Lett.*, **145**(3), pp. 851–859 (2015).

48. Jiang, Y.W., Chai, K., Wang, Y.Q., et al. "Mesoporous silica-supported $CuCo2O_4$ mixed-metal oxides for the aerobic oxidation of alcohols", *ACS Appl. Nano Mater.*, **2**(7), pp. 4435–4442 (2019).

Biographies

Pouya Ghamari Kargar was born in Mashhad, Iran in 1992. He received his BSc degree in Chemistry from Quchan Islamic Azad University in 2014 and MS degree from Shahrood University of Technology in 2016. Now, he received his PhD degree in Organic Chemistry in the Research Laboratory of Green Organic Synthesis & Catalyst under the supervision of Associate Professor Ghodsieh Bagherzade at the Department of Chemistry at University of Birjand. His current research focuses on the rational design of metal-organic framework, magnetic nanoparticles, ionic liquids, nanocomposite, and di and trinuclear catalyst materials for catalysis in the synthesis of organic compounds.

Majid Ghasemi was born in Boshrouyeh, Iran in 1993. He received his BSc in Chemistry from Farhangian University in 2017. Now, he is the MSc candidate in Organic Chemistry with the Research Laboratory of Green Organic Synthesis and Catalyst under the supervision of Associate Professor Dr. Ghodsieh Bagherzade at the Department of Chemistry at the University of Birjand. His current research focuses on the rational design of magnetic nanoparticle materials for catalysis in the synthesis of organic compounds.

Ghodsieh Bagherzade is a Professor at the Chemistry Department of Birjand University. He obtained his PhD degree in Organic Chemistry from Ferdowsi University in 2005. His research interest is mainly focused on the synthesis of multifunctional heterogeneous catalysts for catalytic transformation in a green medium.